Reprint from APPLIED PHYSICS LETTERS 97 (2010) 151914

Diluted manganese on the bond-centered site in germanium

S. Decoster* and A. Vantomme
Instituut voor Kern- en Stralingsfysica and INPAC,K.U.Leuven, Celestijnenlaan 200D, 3001 Leuven, Belgium

S. Cottenier
Center for Molecular Modeling, Ghent University,Technologiepark 903, 9052 Zwijnaarde, Belgium

U. Wahl and J. G. Correia
Instituto Tecnológico e Nuclear, Estrada Nacional 10, 2686-953 Sacavém, Portugal, and
Centro de Física Nuclear da Universidade de Lisboa, Avenida Professor Gama Pinto 2, 1649-003 Lisboa, Portugal

L. M. C. Pereira
Instituut voor Kern- en Stralingsfysica and INPAC, K.U.Leuven, Celestijnenlaan 200D, 3001 Leuven, Belgium
Instituto Tecnológico e Nuclear, Estrada Nacional 10, 2686-953 Sacavém, Portugal, and
IFIMUP and IN-Institute of Nanoscience and Nanotechnology, Departamento de Física, Faculdade de Ciências, Universidade do Porto, 4169-007 Porto, Portugal

C. Lacasta
Instituto de Física Corpuscular IFIC/CSIC-UVEG, PO Box 22085, 46071 Valencia, Spain

M. R. Da Silva
Centro de Física Nuclear da Universidade de Lisboa, Avenida Professor Gama Pinto 2, 1649-003 Lisboa, Portugal

(Received 8 June 2010; accepted 23 September 2010; published online 15 October 2010)

The functional properties of Mn-doped Ge depend to large extent on the lattice location of the Mn impurities. Here, we present a lattice location study of implanted diluted Mn by means of electron emission channeling. Surprisingly, in addition to the expected substitutional lattice position, a large fraction of the Mn impurities occupies the bond-centered site. Corroborated by ab initio calculations, the bond-centered Mn is related to Mn-vacancy complexes. These unexpected results call for a reassessment of the theoretical studies on the electrical and magnetic behavior of Mn-doped Ge, hereby including the possible role of Mn-vacancy complexes. [DOI: 10.1063/1.3501123]

Manganese-doped germanium is regarded as a promising material for spintronic devices. The Mn_xGe_{1-x} semiconductor system exhibits ferromagnetic behavior between 25 and 116 K, with a Curie temperature increasing linearly with Mn concentration between 0.6% and 3.5%.[1] Shortly after this initial work was published, Cho et al.[2] showed ferromagnetic ordering in $Ge_{0.94}Mn_{0.06}$ close to room temperature (285 K). However, the origin of ferromagnetism in this system, grown with molecular beam epitaxy (MBE) or by Mn implantation, is not yet fully understood and has been related to Mn-rich precipitates, such as Mn_5Ge_3 and $Mn_{11}Ge_8$, as well as to magnetic coupling between diluted Mn impurities.[3–6] The (ferro-) magnetic behavior of diluted Mn atoms is expected to depend on their lattice site, which makes this property crucial for a correct understanding of magnetism in this system.

Despite its importance, literature on the lattice location of (diluted) Mn in Ge is rather scarce. Extended x-ray absorption fine structure measurements have shown evidence of diluted Mn atoms on the substitutional (S) site after ion implantation[7] as well as after magnetron cosputtering.[8] Although the presence of diluted Mn is evidenced in both studies, a large fraction of Mn was incorporated in Mn_5Ge_3 precipitates as well. Ottaviano et al.[7] explicitly indicated that, within the detection limit, no Mn atoms were found on the tetrahedral interstitial (T) site. Li et al.[9] used Rutherford backscattering spectrometry in channeling geometry on low temperature MBE (LT-MBE) grown Mn_xGe_{1-x}, which resulted in the observation of 24% of the Mn atoms on the S site and 12% on the T site, with the remainder (64%) distributed randomly throughout the crystal. It is important to note that this lattice location study was hindered by the presence of Mn-rich nanocolumns. Finally, comparison of valence band spectra with ab initio calculations indicated effective substitutional Mn dilution, even after high fluence ion implantation.[10] Besides these experimental studies, several *ab initio* calculations have been performed to determine the heat of formation of Mn on different lattice sites, all of which indicated that Mn prefers the S site to the tetrahedral (T) or hexagonal (H) interstitial site.[11–13]

Here, we present an electron emission channeling (EC) online experiment in combination with ab initio calculations, in order to determine the lattice location of implanted diluted Mn atoms in Ge in a direct way. We evidence that a fraction of the diluted Mn atoms are substitutional, as expected. Surprisingly, however, a relatively large fraction of Mn atoms is located on the bond-centered (BC) site, i.e., in the center of two nearest neighbor substitutional sites. These results may potentially have a profound influence on understanding and modeling the (ferro)magnetic behavior of diluted Mn atoms in Ge. Moreover, it is suggested that the attempts to understand the behavior of Mn in Ge, based on substitutional Mn only, need to be revisited.

EC makes use of the fact that charged particles (in this case electrons), emitted from implanted radioactive isotopes, are guided by the potential of atomic rows and planes while traveling through a single crystal. The resulting anisotropic electron emission patterns around low-index crystal directions are characteristic for the lattice site occupied by the emitting atom and are measured with a two-dimensional energy- and position-sensitive Si detector of 22×22 pixels. This technique has been successfully applied previously, determining the lattice location of a range of impurities in several single crystalline matrices, including Ge,[14–17] reaching an unprecedented

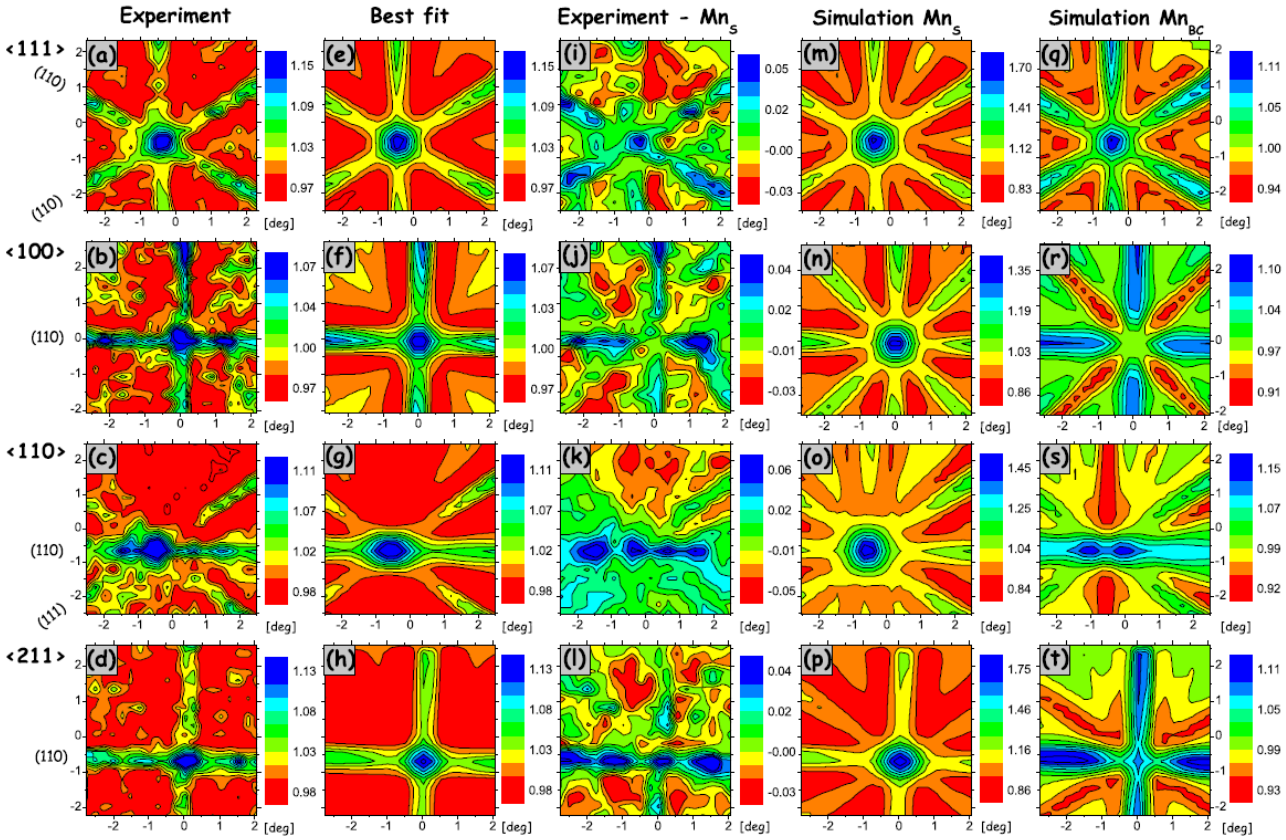

FIG. 1. (Color online) [(a)–(d)] Normalized experimental electron emission patterns around the <111>, <100>, <110>, and <211>-axes in Ge after ^{56}Mn implantation; [(e)–(h)] best fits to the experimental patterns, assuming 37(7)% on the S site and 59(8)% on the BC site; [(i)–(l)] the experimental patterns after subtracting the substitutional fraction; [(m)–(p)] simulated patterns for Mn on the S site and [(q)–(t)] on the BC site.

accuracy as low as 0.1 Å for very low impurity concentrations (< parts per million). More details on EC can be found in Ref. 18 and references therein.

We implanted undoped <111>-Ge with the radioactive ^{56}Mn isotope, which emits β-electrons with an end-point energy of 2.85 MeV and decays to ^{56}Fe with a half life of 2.58 h. The 50 keV implantations have been performed at the ISOLDE facility in CERN. Since Ge is known to be highly sensitive to (ion) irradiation,[19] the implantation was performed at an elevated temperature of 300 °C in order to minimize lattice damage in the Ge single crystal. An offset angle with respect to the surface normal was used to minimize ion channeling during implantation. The implantation fluence was kept below 5×10^{12} atoms/cm^2, to minimize Mn-clustering and to assure good dilution ($<10^{18}$ /cm^3) of the Mn atoms in the Ge matrix. The EC measurements have been performed in situ, in a vacuum of $<10^{-5}$ mbar and at room temperature.

To obtain unambiguous quantitative results, the electron emission patterns are measured around four independent crystal directions, analyzed consistently, and fitted to a set of simulated patterns. These simulations are based on the dynamical theory of electron diffraction,[20] and patterns were calculated for the S, T, BC, H, and the so-called SP, Y, and C sites, as well as for discrete displacements between all of these high-symmetry sites along the <111>- and <100>-directions. A schematic representation of these high-symmetry sites in a diamond lattice can be found in Ref. 21. The normalized electron emission patterns around the <111>, <100>, <110>, and <211> directions are shown in Fig. 1 in panels (a)–(d), respectively. The high normalized electron yield in the center of the patterns indicates that at least a fraction of the implanted Mn ions occupies the S site. However, when visually comparing the experimental patterns in panels (a)–(d) with the simulated patterns for purely substitutional Mn atoms in panels (m)–(p), it is clear that not all of the experimentally observed channeling and blocking effects can be reproduced when only assuming substitutional Mn. This strongly indicates that more than one high-symmetry site is involved. For clarification, we have subtracted the substitutional contribution from the experimental patterns, resulting in panels (i)–(l). The anisotropy in these patterns is a visual proof of the fact that a fraction of the Mn impurities occupy other high-symmetry sites as well. In order to obtain accurate quantitative information, and in order to determine the occupied lattice sites, we have performed a thorough fitting procedure,[18] where Mn was allowed to occupy up to four different lattice sites - making all possible combinations of the S, T, BC, AB, H, Y, C, and SP sites as well as discrete displacements in between all of these sites. From this study, it could be concluded that the only fit which is consistent in all four crystal directions and results in a significant fit improvement, is obtained by assuming Mn on two high-symmetry sites: 37(7)% of the Mn atoms on the S site and 59(8)% on a slightly displaced (~0.25 Å) BC site. These best fits to the experimental patterns are shown in panels (e)–(h), from which it can be visually inspected that all experimentally observed axial and planar channeling and locking effects are well reproduced. Moreover, it is clear hat the simulated patterns for Mn on the BC site in panels (q)–(t) have a similar anisotropy as the experimental patterns fter subtraction of the substitutional contribution in

panels (i)–(l), which shows that a fraction of the Mn impurities are indeed located on the BC site.

The occupation of the substitutional site by diluted Mn atoms is in agreement with literature.[7–13] However, the observation of an even larger fraction of Mn atoms on the BC site is much more striking. In recent EC experiments, the transition metals Fe, Cu, and Ag have also been observed on the BC site.[15] Ab initio calculations indicated that these impurities on the BC site are related to impurity-vacancy complexes in the so-called split-vacancy configuration,[15] i.e., with the impurity on the BC site, in the center of two nearest neighbor vacant sites. In order to understand the reason why Mn atoms appear on the BC site, ab initio calculations similar to the ones in Ref. 15 were performed, using the augmented plane wave and local orbitals method within density functional theory, as implemented in the WIEN2K code. First of all, these calculations have evidenced that the Mn-vacancy complex with Mn on the S site and a vacancy as nearest neighbor is unstable and relaxes toward the split-vacancy configuration. We have also calculated the heat of formation[22] of an isolated vacancy in Ge (2.23 eV), of substitutional Mn (2.28 eV) and of the Mn-vacancy complex in the split-vacancy configuration (4.05 eV). Hence, the heat of formation of Mn in the split-vacancy configuration is significantly smaller than the sum of the heats of formation of substitutional Mn and an isolated vacancy (4.51 eV). These results indicate that vacancies, which are abundantly available during implantation and which are highly mobile at 300 °C,[23] are very likely to be trapped by the substitutional Mn impurities, which will spontaneously relocate toward the BC site. These results can be interpreted as a model to induce lattice site changes of the Mn atoms, i.e., by introducing vacancies (e.g., by electron irradiation), the substitutional impurities are relocated to the BC site.

Our calculations indicate that, after full lattice relaxation, Mn occupies an undisplaced BC site after trapping a vacancy, while the best fit of the EC patterns was obtained with a slightly displaced (~0.25 Å) BC site. From the presented experiments, however, it is not possible to unambiguously determine the origin of this displacement. It is possible that all of the Mn atoms in the near-BC fraction are located on a site which is ~0.25 Å displaced from an ideal BC site toward a nearest neighbor S site but we believe that the observed BC fraction is a mixture of Mn atoms on the undisplaced BC site (in the split-vacancy configuration) and on a displaced BC site. The Mn atoms on a displaced BC site are most likely related to more complex defect configurations, e.g., involving more than one vacancy.

It is clear that the presence of vacancies drastically influences the occupied lattice sites of diluted Mn in Ge. When vacancies are abundantly available, which is the case during ion implantation, a high fraction of substitutional Mn atoms gets relocated to the BC site. Moreover, also during MBE growth of Mn_xGe_{1-x} layers, a large number of vacancies can be expected, especially when LT-MBE (<85 °C) growth is used in order to prevent the formation of Mn-rich precipitates.[4] Hence, it can be expected that at least a fraction of the diluted Mn atoms occupy the BC site, both in ion implanted and in LT-MBE grown Mn_xGe_{1-x} samples.

It is important to note that, within the detection limit of the EC experiment (<3%), the implanted Mn atoms do not occupy the T or the H interstitial site. This result, in combination with the observation of Mn on the BC site, calls for revisiting the generally accepted picture about the lattice location of diluted Mn atoms in Ge. In particular, several models that implicitly rely on the occurrence of Mn on the S, T, or H site need to be reconsidered. Examples are the determination of exchange constants for the Mn–Mn magnetic interaction in Ge,[1,24] and the determination of electric and magnetic properties of diluted Mn in Ge.[11–13] The current results indicate that in order to fully comprehend the electrical and magnetic behavior of this diluted magnetic semiconductor system, additional theoretical studies, which also consider Mn on the BC site in the split-vacancy configuration, are highly recommended.

We acknowledge the technical support from A.C. Marques, P. Weilhammer, and E. Chesi. This work was supported by the Research Foundation, Flanders (FWO G.0501.07, G.0636.08), the K.U.Leuven projects GOA/2009/006 and INPAC EF/2005/005, the IUAP P6/42 Program, the EURONS project (RII3-CT-2004-506065), and the Portuguese Foundation for Science and Technology (Grant Nos. SFRH/BD/35761/2007 and CERN/FP/109272/2009).

* Electronic mail: stefan.decoster@fys.kuleuven.be.

[1]Y.D. Park, A.T. Hanbicki, S.C. Erwin, C.S. Hellberg, J.M. Sullivan, J.E. Mattson, T.F. Ambrose, A. Wilson, G. Spanos, and B. T. Jonker, Science 295, 651 (2002).
[2]S. Cho, S. Choi, S.C. Hong, Y. Kim, J.B. Ketterson, B.-J. Kim, Y.C. Kim, and J.-H. Jung, Phys. Rev. B 66, 033303 (2002).
[3]F. D'Orazio, F. Lucari, M. Passacantando, P. Picozzi, S. Santucci, and A. Verna, IEEE Trans. Magn. 38, 2856 (2002).
[4]A.P. Li, J. Shen, J.R. Thompson, and H.H. Weitering, Appl. Phys. Lett. 86, 152507 (2005).
[5]S. Ahlers, D. Bougeard, N. Sircar, G. Abstreiter, A. Trampert, M. Opel, and R. Gross, Phys. Rev. B 74, 214411 (2006).
[6]E. Biegger, L. Stäheli, M. Fonin, U. Rüdiger, and Y. S. Dedkov, J. Appl. Phys. 101, 103912 (2007).
[7]L. Ottaviano, M. Passacantando, A. Verna, R. Gunnella, E. Principi, A. DiCicco, G. Impellizzeri, and F. Priolo, J. Appl. Phys. 100, 063528 (2006).
[8]J. Ye, Y. Jiang, Q. Liu, Y. Sun, Z. Pan, and S. Wei, J. Phys.: Conf. Ser. 190, 012104 (2009).
[9]A.P. Li, C. Zeng, K. van Benthem, M. F. Chisholm, J. Shen, S.V.S. Nageswara Rao, S.K. Dixit, L.C. Feldman, A.G. Petukhov, M. Foygel, and H.H. Weitering, Phys. Rev. B 75, 201201(R) (2007).
[10]L. Ottaviano, M. Passacantando, S. Picozzi, A. Continenza, R. Gunnella, A. Verna, G. Bihlmayer, G. Impellizzeri, and F. Priolo, Appl. Phys. Lett. 88, 061907 (2006).
[11]X. Luo, S.B. Zhang, and S.-H. Wei, Phys. Rev. B 70, 033308 (2004).
[12]Z.Z. Zhang, B. Partoens, K. Chang, and F.M. Peeters, Phys. Rev. B 77, 155201 (2008).
[13]A. Continenza, G. Profeta, and S. Picozzi, Phys. Rev. B 73, 035212 (2006).
[14]S. Decoster, B. De Vries, U. Wahl, J.G. Correia, and A. Vantomme, Appl. Phys. Lett. 93, 141907 (2008).
[15]S. Decoster, S. Cottenier, B. De Vries, H. Emmerich, U. Wahl, J.G. Correia, and A. Vantomme, Phys. Rev. Lett. 102, 065502 (2009).
[16]S. Decoster, B. De Vries, U. Wahl, J. G. Correia, and A. Vantomme, J. Appl. Phys. 105, 083522 (2009).
[17]S. Decoster, S. Cottenier, U. Wahl, J.G. Correia, and A. Vantomme, Phys. Rev. B 81, 155204 (2010).
[18]U. Wahl, J.G. Correia, A. Czermak, S.G. Jahn, P. Jalocha, J.G. Marques, A. Rudge, F. Schopper, J.C. Soares, A. Vantomme, P. Weilhammer, and ISOLDE Collaboration, Nucl. Instrum. Methods Phys. Res. A 524, 245 (2004).
[19]S. Decoster and A. Vantomme, J. Phys. D 42, 165404 (2009).
[20]H. Hofsäss and G. Lindner, Phys. Rep. 201, 121 (1991).
[21]U. Wahl, J.G. Correia, A. Vantomme, G. Langouche, and ISOLDE Collaboration, Physica B 273–274, 367 (1999).
[22]The equation used to calculate the heat of formation is fully explained in Ref. 15, with the only difference that the chemical potential μ_{imp} is based on antiferromagnetic bcc-Mn.
[23]H. Haesslein, R. Sielemann, and C. Zistl, Phys. Rev. Lett. 80, 2626 (1998).
[24]Y.-J. Zhao, T. Shishidou, and A.J. Freeman, Phys. Rev. Lett. 90, 047204 (2003).